Determination of piezooptic coefficient π_{14} of $LiNbO_3$ crystals under torsion loading

Vasylkiv Yu., Savaryn V., Smaga I., Skab I. and Vlokh R.

Institute of Physical Optics, 23 Dragomanov St., 79005, Lviv, Ukraine, vlokh@ifo.lviv.ua

Received: 29.06.2010

Abstract

We show that non-principal piezooptic coefficients can be quite accurately determined after a distribution of shear strain components under torsion of $LiNbO_3$ crystal rod has been studied. The piezooptic coefficient π_{14} of $LiNbO_3$ crystals found in this way is $|\pi_{14}| = (8.87 \pm 0.28) \times 10^{-13}\,\mathrm{m}^2/\mathrm{N}$, while the corresponding error is very low and amounts to 3.1%.

Keywords: piezooptic coefficients, lithium niobate crystals, methods of measurements, torsion strains

PACS: 78.20.Hp, 62.20.-x
UDC: 535.542

1. Introduction

The piezooptic effect consists in changes of optical impermeability coefficients ΔB_{ij} (or refractive indices $B_{ij} = (1/n^2)_{ij}$) of a medium under the action of mechanical strains σ_{kl}. It can be described by the relation

$$\Delta B_{ij} = B_{ij} - B_{ij}^0 = \pi_{ijkl}\sigma_{kl}\,, \tag{1}$$

where π_{ijkl} is a fourth rank piezooptic tensor, and B_{ij} and B_{ij}^0 denote impermeability tensors of strained and mechanically free samples, respectively. Usually this effect is studied while applying to samples homogeneous mechanical stresses.

It is well known (see, e.g., [1]) that the piezooptic coefficients are usually measured with a high error which can exceed 30%. This error is caused by misalignments of loading and, what is more important, by a so called barrel-shaped distortion that appears due to a friction force existing among sample faces, a cover cap and a substrate, which are used for sample loading. As a result, the distribution of stresses inside a sample is generally unknown. In order to determine the piezooptic coefficients more precisely, a so-called three-point bend technique is often used [2]. Then the distribution of stresses inside the sample is determined in advance. The same should be true for the application of torsion moment to the sample. Moreover, using of the torsion seems to be advantageous since it enables determining the piezooptic coefficients which usually cannot be measured due to a complicated experimental geometry or which should be recalculated in a

cumbersome way from the indirect measurement results [3, 4], thus leading to increasing error that can exceed typical mean values of the piezooptic coefficients. The components of the piezooptic tensor belonging to this type are $\pi_{\lambda\mu}$ (in the matrix notation), where $\lambda = 1, 2, ...6$ and $\mu = 4, 5, 6$.

As shown in our earlier works [5–9], the application of torsion [5, 6, 8, 9] or bending [6, 7, 9] stresses would lead to specific distributions of the optical birefringence and the optical indicatrix rotation in crystals. Under the torsion around a *Z* axis, a special point of zero induced birefringence has been revealed in the geometrical centre of a sample of *XY* cross section, which corresponds to a zero shift stress components σ_{13} and σ_{23}. This point lies on the torsion axis. It has been found that the birefringence increases linearly with increasing distance from the geometrical centre of the *XY* cross section of a sample. Moreover, it has been shown that the birefringence distribution forms a conical surface in the coordinates $(X, Y, \Delta n)$ [1, 2]. A single-laser beam polarimetric technique has been used in those experiments, involving a beam scanning across *XY*-face of a sample. This technique has a low resolution limited by a laser beam diameter and so it could be successfully replaced with a method of imaging polarimetry.

When a torsion deformation around *Z* axis is applied to a cylindrical sample, the strain tensor components may be defined as [10]:

$$\sigma_\mu = \frac{2M_z}{\pi R^4}(X\delta_{4\mu} - Y\delta_{5\mu}), \tag{2}$$

where $M_z = \int_S r \times PdS$, $\delta_{4\mu}$, $\delta_{5\mu}$ is the Kronecker delta, *R* the cylinder radius, *S* the square of the cylinder basis, and *P* the stress. Therefore we deal with two shear components of the stress tensor, σ_{32} and σ_{31}:

$$\sigma_4 = \sigma_{32} = \frac{2M_z}{\pi R^4}X \tag{3}$$

and

$$\sigma_5 = \sigma_{31} = \frac{2M_z}{\pi R^4}Y, \tag{4}$$

which linearly depend on the coordinates. The latter dependences enable one to determine unambiguously a distribution of shear strain tensor components inside a sample under study. Moreover, application of the torsion moment can provide purely tangential displacements (or shear strain components), which otherwise (i.e., under other geometries of sample loading) are usually accompanied by normal displacements, thus leading to simultaneous appearance of compression and/or extension strain components. Actually, a situation in which many strain components simultaneously appear in the same experiment triggers a necessary consideration of many complicated relationships among whole sets of piezooptic tensor components and mechanical strains. In its turn, this is one of the reasons for increasing typical errors of determination of particular piezooptic coefficients.

As a consequence of the above consideration, the present work is devoted to analysis of the conditions under which a non-principle piezooptic tensor component π_{14} can be determined using a torsion deformation of $LiNbO_3$ crystals.

2. Experimental

$LiNbO_3$ crystals belong to the point symmetry group $3m$. The crystal used in our experiment was prepared as an octahedral prism, with its lateral faces being parallel to Z axis (see Fig. 1) and the basis parallel to XY plane. The sample had a length of 13 mm along the Z axis and a distance of 6 mm between the lateral faces. YZ plane was accepted to be parallel to one of the symmetry mirror planes. The light of a He-Ne laser (the wavelength of $\lambda = 632.8$ nm) propagated along the Z axis which represents an optic axis of the crystal.

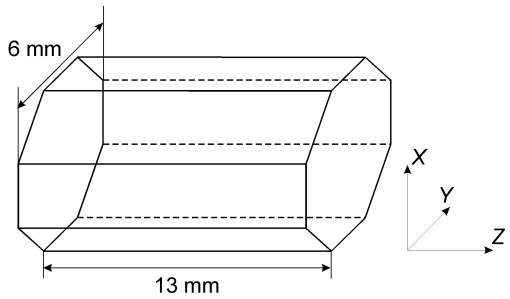

Fig. 1. Shape and orientation of $LiNbO_3$ crystal sample.

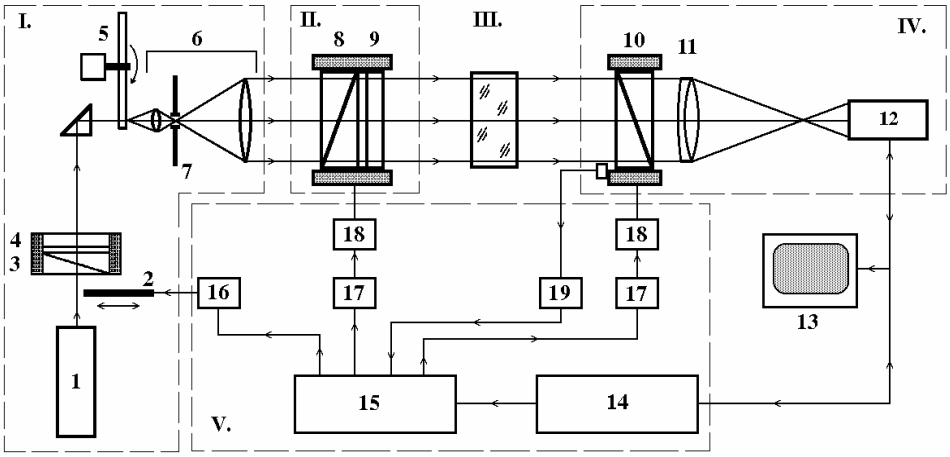

Fig. 2. Schematic representation of the imaging polarimeter (I – light source section; II – polarisation generator; III – specimen section; IV – polarisation analyser; and V – controlling unit): 1 – He-Ne laser; 2 – ray shutter; 3, 8 – polarisers; 4, 9 – quarter-wave plates; 5 – coherence scrambler; 6 – beam expander; 7 – spatial filter; 10 – analyser; 11 – objective lens; 12 – CCD camera; 13 – TV monitor; 14 – frame grabber; 15 – PC; 16 – shutter's controller; 17 – step motors' controllers; 18 – step motors; 19 – reference position controller.

A torsion moment M_z was applied to one of the basic faces of a crystalline prism, while the opposite basic face was kept fixed. An experimental setup for birefringence measurements is shown in Fig. 2. While studying the optical birefringence, we exploited an imaging polarimetric setup described elsewhere (see [11] and Fig. 2). The only minor modifications were that a quarter-wave plate (a component 9 in Fig. 2) was removed from polarisation generator and that linearly polarised incident light was used. The rotation stage angles corresponding to minimums of transmitted light intensity detected by a CCD camera were ascribed to the extinction positions. The optical birefringence was studied with a Senarmont technique. In this case the quarter wave plate was placed behind the sample. The birefringence has been calculated following from the formula $\Delta n = \beta\lambda / \pi d$, where β is the rotation angle of polarisation plane behind the quarter wave plate with respect to the initial position and d the specimen thickness along the direction of light propagation.

3.Experimental results

Distributions of the birefringence induced by the torsion moment $M_z = 63.77 \times 10^{-3}$ N×m along the X and Y axes and the bisector of the X and Y axes are presented in Fig. 3. These dependences are linear, at least for the distances less than ~ 2 mm from the torsion axis. A deviation from the linear dependence is observed for larger distances. It could be explained by both the influence of sample boundaries and a deviation of the sample shape from the cylindrical one.

The piezooptic tensor for the point symmetry group 3m is as follows:

	σ_{11}	σ_{22}	σ_{33}	σ_{32}	σ_{31}	σ_{21}
ΔB_{11}	π_{11}	π_{12}	π_{13}	π_{14}	0	0
ΔB_{22}	π_{11}	π_{11}	π_{13}	$-\pi_{14}$	0	0
ΔB_{33}	π_{31}	π_{31}	π_{33}	0	0	0
ΔB_{32}	π_{41}	$-\pi_{41}$	0	π_{44}	0	0
ΔB_{31}	0	0	0	0	π_{44}	$2\pi_{41}$
ΔB_{21}	0	0	0	0	π_{14}	π_{66}

. (5)

Then the equation of the optical indicatrix perturbed by the two shear strains reads as

$$(B_{11} + \pi_{14}\sigma_{32})X^2 + (B_{11} - \pi_{14}\sigma_{32})Y^2 + B_{33}Z^2 + 2\pi_{44}\sigma_{32}YZ + 2\pi_{44}\sigma_{31}XZ + 2\pi_{14}\sigma_{31}XY = 1. \quad (6)$$

Now let us consider the birefringence induced by the torsion. Using Eqs. (3) and (4), one can represent the coordinate dependences of the birefringence as dependences on the strain tensor components (see Fig. 3). For example, we have the strain component $\sigma_{31} = 0$ in the $Y = 0$ plane and so the optical indicatrix equation is given by

$$(B_{11} + \pi_{14}\sigma_{32})X^2 + (B_{11} - \pi_{14}\sigma_{32})Y^2 + B_{33}Z^2 + 2\pi_{44}\sigma_{32}YZ = 1 \quad (7)$$

(see Fig. 3a). Then the cross section of the Fresnel ellipsoid by the plane orthogonal to the direction of optical wave propagation (i.e., the section by the plane $Z = 0$) is easily found as

$$(B_{11} + \pi_{14}\sigma_{32})X^2 + (B_{11} - \pi_{14}\sigma_{32})Y^2 = 1. \quad (8)$$

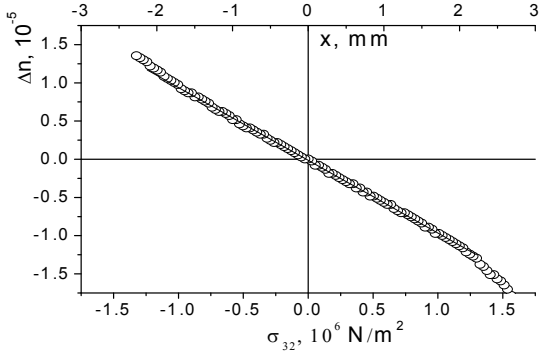

(a)

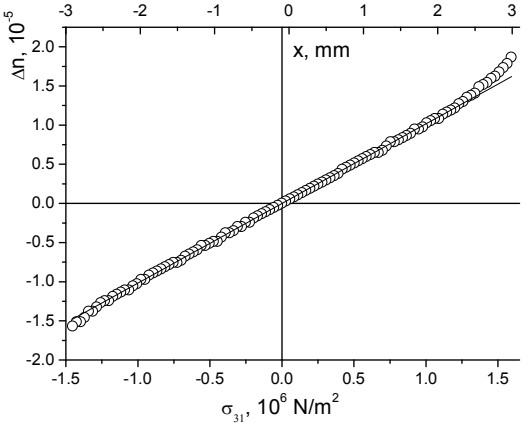

(b)

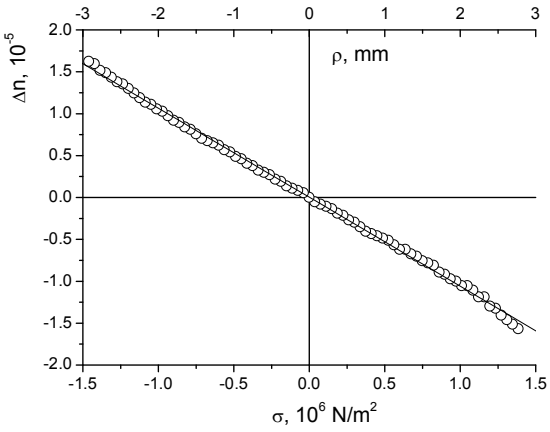

(c)

Fig. 3. Distribution of birefringence induced by the torsion moment $M_z = 63.77 \times 10^{-3}$ N×m (a) along the *X* axis, (b) the *Y* axis and (c) the bisector of the *X* and *Y* axes: circles are the experimental data and solid lines the linear fitting. A scale corresponding to the shear strain component is also shown.

The principle values of the refractive indices in the XY plane and the corresponding birefringence are defined by the relations

$$n_1 = n_0 + \frac{1}{2} n_0^3 \pi_{14} \sigma_{32} = n_0 + n_0^3 \pi_{14} \frac{M_z}{\pi R^4} X,$$
$$n_2 = n_0 - \frac{1}{2} n_0^3 \pi_{14} \sigma_{32} = n_0 - n_0^3 \pi_{14} \frac{M_z}{\pi R^4} X, \qquad (9)$$
$$\Delta n = n_0^3 \pi_{14} \sigma_{32} = n_0^3 \pi_{14} \frac{2M_z}{\pi R^4} X,$$

where n_0 is the initial ordinary refractive index.

The results presented in Fig. 3a correspond exactly to Eqs. (9). Thus, the piezooptic coefficient may be determined as

$$|\pi_{14}| = \frac{\Delta n}{n_0^3 \sigma_{32}}, \qquad (10)$$

where the refractive index is equal to $n_o = 2.28647$ at the wavelength of 632.8 nm [12].

For the $X = 0$ plane one has the component $\sigma_{32} = 0$ (see Fig. 3b). As a result, the XY cross section of the optical indicatrix given by Eq. (7) reduces to

$$B_{11} X^2 + B_{11} Y^2 + 2\pi_{14} \sigma_{31} XY = 1, \qquad (11)$$

where

$$|\pi_{14}| = \frac{\Delta n}{n_0^3 \sigma_{31}}. \qquad (12)$$

For the case of light propagation along the bisector ρ of the X and Y axes (see Fig. 3c) one can obtain the following relation determining the birefringence value:

$$\Delta n = n_0^3 \pi_{14} \sqrt{2} \sigma, \qquad (13)$$

while the relation for the piezooptic coefficient is given by

$$|\pi_{14}| = \frac{\Delta n}{n_0^3 \sqrt{2} \sigma}. \qquad (14)$$

The values of the piezooptic coefficient calculated following from the data presented above are $|\pi_{14}| = (8.36 \pm 0.02) \times 10^{-13}\,\mathrm{m}^2/\mathrm{N}$ (Eq. (10), $|\pi_{14}| = (8.92 \pm 0.02) \times 10^{-13}\,\mathrm{m}^2/\mathrm{N}$ (Eq. (12)) and $|\pi_{14}| = (9.33 \pm 0.04) \times 10^{-13}\,\mathrm{m}^2/\mathrm{N}$ (Eq. (14)). These values turn out to be close enough, with the mean coefficient being equal to $|\pi_{14}| = (8.87 \pm 0.28) \times 10^{-13}\,\mathrm{m}^2/\mathrm{N}$.

Hence, the results of our experiment show that we deal with a precise enough technique for measuring non-principal piezooptic coefficients such as π_{14}. Namely, the torsion method suggested by us represents a new and precise technique for determining the piezooptic coefficients, with the error as small as 3.1%. Notice that the value of the π_{14} coefficient derived by us agrees satisfactorily with that obtained in a number of other works with the interferometric techniques (e.g., $\pi_{14} = 0.7 \times 10^{-12}\,\mathrm{m}^2/\mathrm{N}$ [13] and

$\pi_{14} = -0.81 \times 10^{-12}\,\mathrm{m}^2/\mathrm{N}$ [14]), though the relative errors of the latter is notably larger (15%, according to the estimations [14]). In other words, the accuracy of our technique is much higher than that presented in [14]. Here we should stress that determination of the sign of piezooptic coefficients does not represent a goal of this work. Nonetheless, this would be quite possible to accomplish in frame of our technique while verifying additionally the sign of the birefringence induced by the shear strains of predefined signs.

It seems reasonable to consider in a more detail the following components of the strain tensor appearing under torsion of $LiNbO_3$, which can lead to photoelastic coupling:

$$\begin{aligned} e_{11} &= \frac{2M_z}{\pi R^4} S_{14} X,\ e_{22} = -\frac{2M_z}{\pi R^4} S_{14} X,\ e_{33} = 0, \\ e_{32} &= \frac{2M_z}{\pi R^4} S_{44} X,\ e_{31} = \frac{2M_z}{\pi R^4} S_{55} Y,\ e_{12} = \frac{4M_z}{\pi R^4} S_{14} Y. \end{aligned} \tag{15}$$

According to Eqs. (15), five components of the strain tensor remain non-zero when the $LiNbO_3$ crystals are being under torsion deformation around the Z axis. Let us write down the appropriate optical indicatrix perturbations separately for the $X = 0$ and $Y = 0$ planes:

$$\begin{aligned} B_{11}X^2 + B_{11}Y^2 + B_{33}Z^2 + 2p_{44}e_{13}ZX + 2p_{41}e_{12}ZX + \\ 2p_{14}e_{13}XY + 2p_{66}e_{12}XY = 1, \end{aligned} \tag{16}$$

and

$$\begin{aligned} (B_{11} + p_{11}e_{11} + p_{12}e_{22} + p_{14}e_{32})X^2 + (B_{11} + p_{12}e_{11} + p_{11}e_{22} - p_{14}e_{32})Y^2 \\ + B_{33}Z^2 + 2p_{41}e_{11}ZY - 2p_{41}e_{22}ZY + 2p_{14}e_{32}ZY = 1, \end{aligned} \tag{17}$$

where p_{ij} are the photoelastic coefficients. The cross sections of these ellipsoids by the $Z = 0$ plane take the following forms:

$$B_{11}X^2 + B_{11}Y^2 + 2p_{14}e_{13}XY + 2p_{66}e_{12}XY = 1, \tag{18}$$

and

$$(B_{11} + p_{11}e_{11} + p_{12}e_{22} + p_{14}e_{32})X^2 + (B_{11} + p_{12}e_{11} + p_{11}e_{22} - p_{14}e_{32})Y^2 = 1. \tag{19}$$

The principal refractive indices and the birefringence determined from Eqs. (16) and (19) are given by

$$\begin{aligned} n_{1,2} &= n_0 \pm \frac{1}{2} n_0^3 (p_{14}e_{13} + p_{66}e_{12}) \\ \Delta n &= n_0^3 (p_{14}e_{13} + p_{66}e_{12}) = 2n_0^3 (p_{14}S_{55} + 2p_{66}S_{14}) \frac{M_z}{\pi R^4} Y \end{aligned} \tag{20}$$

Eqs. (20) yield in the principle refractive indices

$$\begin{aligned} n_1 &= n_0 + \frac{1}{2} n_0^3 (p_{11}e_{11} + p_{12}e_{12} + p_{14}e_{32}), \\ n_2 &= n_0 + \frac{1}{2} n_0^3 (p_{12}e_{11} + p_{11}e_{12} - p_{14}e_{32}). \end{aligned} \tag{21}$$

Then the corresponding birefringence may be found as

$$\Delta n = \frac{1}{2} n_0^3 \left[(p_{11} - p_{12})(e_{11} - e_{22}) + 2 p_{14} e_{32} \right]. \quad (22)$$

Accounting for Eq. (16) and the relations $p_{66} = (p_{11} - p_{12})/2$ and $S_{44} = S_{55}$, one can represent Eq. (22) as

$$\Delta n = 2 n_0^3 (p_{14} S_{55} + 2 p_{66} S_{14}) \frac{M_z}{\pi R^4} X. \quad (23)$$

Thus, Eqs. (20) and (23) are similar and the dependences of the birefringence on the X and Y coordinates are the same. Using these relations, one can determine the sum of the photoelastic coefficients:

$$p_{14} S_{44} + 2 p_{66} S_{14} = \frac{\Delta n \pi R^4}{2 M_z X n_0^3}. \quad (24)$$

The elastic compliance coefficients for the lithium niobate crystals depend essentially on the electric conditions of samples and are equal to $S_{44}^E = 17.0 \times 10^{-12}\,\mathrm{m}^2/\mathrm{N}$, $S_{14}^E = -1.02 \times 10^{-12}\,\mathrm{m}^2/\mathrm{N}$ and $S_{44}^D = 10.8 \times 10^{-12}\,\mathrm{m}^2/\mathrm{N}$ and $S_{14}^P = 0.87 \times 10^{-12}\,\mathrm{m}^2/\mathrm{N}$ [15]. In our experiments we have used no action in order to electrically shorten the sample, so that the elastic compliances determined under constant field conditions should be used while estimating the photoelastic coefficients. It has been found that $17.0 p_{14} - 2.04 p_{66} = |0.31|$. This result in fact disagrees with the data [16]. Indeed, when using the values $p_{11} = -0.02$, $p_{12} = 0.08$, $p_{66} = 0.05$, $p_{14} \simeq -0.08$ [16], one can calculate $17.0 p_{14} - 2.04 p_{66} = |1.26|$, though the photoelastic data reported in [16] are scattered much. Actually, the disagreement mentioned above may be, most probably, caused by non-controlled electrical conditions of samples in the experiments reported in [16] and in our studies.

4.Conclusions

Following from the effect of torsions on the optical birefringence measured for the $LiNbO_3$ crystals, we have testified that the appropriate experiment can be used for precise determination of some of the piezooptic coefficients. Namely, we have shown that the exact measurements of spatial distribution of the shear strain components, under the conditions of twisted rod of crystal, may serve as a technique for determining the non-principal piezooptic coefficients. The piezooptic coefficient π_{14} of $LiNbO_3$ crystals has been found ($|\pi_{14}| = (8.87 \pm 0.28) \times 10^{-13}\,\mathrm{m}^2/\mathrm{N}$) with a very low error (3.1%) which is far less than the typical errors of piezooptic measurements. The photoelastic coefficients of $LiNbO_3$ crystals have also been estimated.

References

1. Vasylkiv Yu, Kvasnyuk O, Krupych O, Mys O, Maksymuk O and Vlokh R, 2009. Reconstruction of 3D stress fields basing on piezooptic experiment. Ukr. J. Phys. Opt. **10**: 22–37.

2. Peng H J, Wong S P and Ho H P, 2004. Measurement of orientation dependent stress-optic coefficient of GaAs single crystals. Appl. Phys. Lett. **84**: 1829–1831.
3. Mytsyk B, 2003. Methods for the studies of the piezo-optical effect in crystals and the analysis of experimental data. I. Methodology for the studies of piezo-optical effect. Ukr. J. Phys. Opt. **4**: 1–26.
4. Andrushchak A S, Bobitski Ya V, Kaidan M V, Mytsyk B G, Kityk A V and Schranz W, 2005. Two-fold interferometric measurements of piezo-optic constants: application to β -BaB_2O_4 crystals. Opt. & Laser Techn. **37**: 319–328.
5. Vlokh R O, Pyatak Y A and Skab I P, 1991. The elasto-optic effect in $LiNbO_3$ crystals under the torsion. Fiz. Tverd. Tela. **33**: 2467–2470.
6. Vlokh R, Kostyrko M and Skab I, 1998. Principle and application of crystallo-optical effects induced by inhomogeneous deformation. Japan. J. Appl. Phys. **37**: 5418–5420.
7. Vlokh R, Pyatak Y and Skab I, 1992. Elasto-optic effect in $LiNbO_3$ under the crystal bending. Ferroelectrics. **126**: 239–242.
8. Vlokh R, Kostyrko M and Skab I, 1997. The observation of "neutral" birefringence line in $LiNbO_3$ crystals under torsion. Ferroelectrics. **203**: 113–117.
9. Vlokh R O, Kostyrko M E and Skab I P, 1997. Description of gradients of piezo-gyration and piezo-optics caused by twisting and bending. Crystallogr. Rep. **42**: 1011–1013.
10. Sirotin Yu I and Shaskolskaya M P. Fundamentals of crystal physics. Moscow: Nauka (1979).
11. Vlokh R, Krupych O, Kostyrko M, Netolya V and Trach I, 2001. Gradient thermooptical effect in $LiNbO_3$ crystals. Ukr. J. Phys. Opt. **2**: 154–158.
12. http://www.almazoptics.com/LiNbO3.htm
13. Mytsyk B, 2003. Methods for the studies of the piezo-optical effect in crystals and the analysis of experimental data. II. Analysis of experimental data. Ukr. J. Phys. Opt. **4**: 105–118.
14. Mytsyk B G, Andrushchak A S, Demyanyshyn N M, Kost' Y P, Kityk A V, Mandracci P and Schranz W, 2009. Piezo-optic coefficients of MgO-doped $LiNbO_3$ crystals. Appl. Opt. **48**: 1904–1911.
15. Warner A W, Onoe M, and Coquin G A, 1967. Determination of Elastic and Piezoelectric Constants for Crystals in Class (3m). J.Acoust.Soc.Am. 42: 1223-1231.
16. Wong K K, Properties of lithium niobate. London: INSPEC. The Institute of Electrical Engineers. (2002).

Vasylkiv Yu., Savaryn V., Smaga I., Skab I. and Vlokh R. 2010. Determination of piezooptic coefficient π_{14} of $LiNbO_3$ crystals under torsion loading. Ukr.J.Phys.Opt. 11: 156–164.

Анотація. *В роботі показано, що не основні п'єзооптичні коефіцієнти можуть бути достатньо точно визначені при встановленні розподілу зсувних напружень зумовлених крученням стержня кристалу $LiNbO_3$. Визначений, таким чином, пєзооптичний коефіцієнт π_{14} кристалів $LiNbO_3$ становить $|\pi_{14}| = (8.87 \pm 0.28) \times 10^{-13}\,\mathrm{m^2/N}$, тоді як відповідна похибка вимірювання дорівнює 3.1%.*